Electronic Supplementary Material (ESI) for New Journal of Chemistry.

Supplementary Information

Red emissive carbon dots obtained from direct calcination of 1,2,4-triaminobenzene for dual-mode pH sensing in living cells

Yueyue Chen, Chan Wang*, Yalan Xu, Guoxia Ran, Qijun Song*

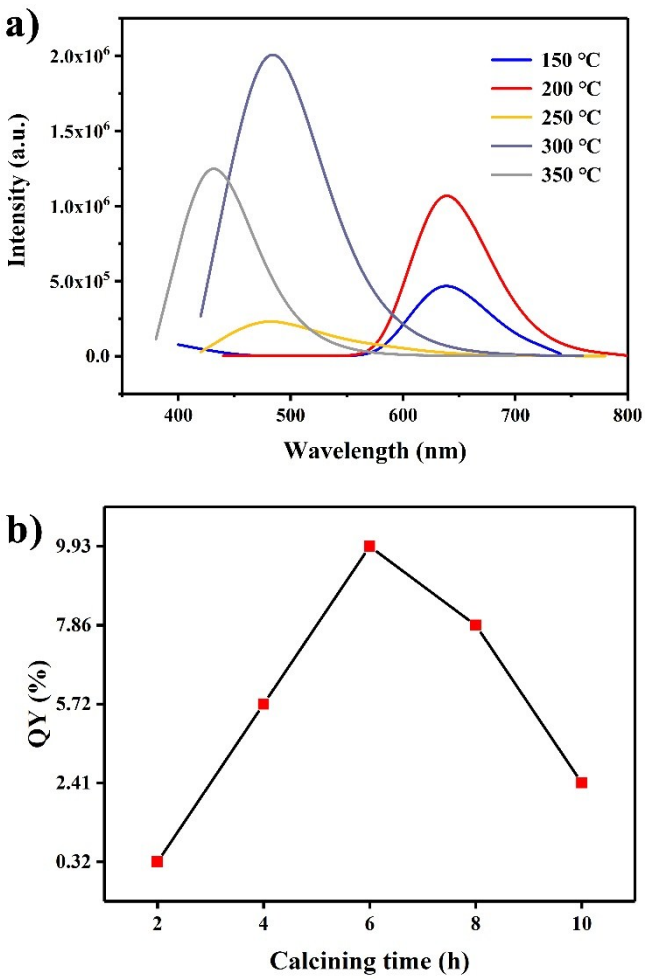

Figure S1. a) Fluorescence emission spectra of r-CDs at different calcining temperature. b) Quantum yields of r-CDs under different calcining time.

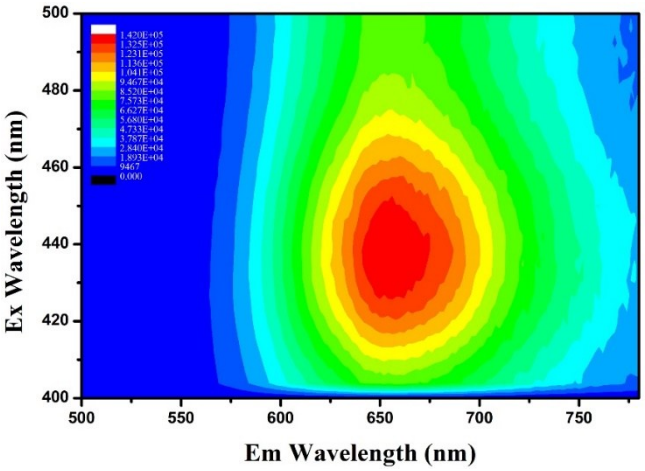

Figure S2. Fluorescence matrix scan of r-CDs during the calcination treatment for 6 h at the temperature of 200 °C.

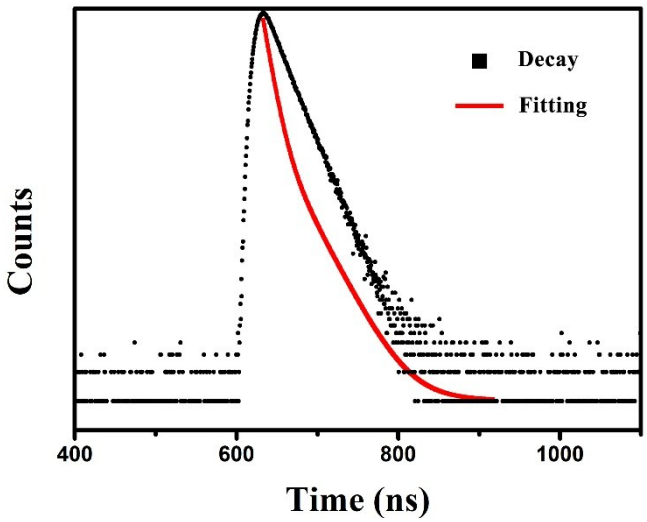

Figure S3. Fluorescence decay curve (black) and its fitting curve (red) of r-CDs during the calcination treatment for 6 h at the temperature of 200 °C.

Table S1. Fluorescence lifetime of r-CDs during the calcination treatment for 6 h at the temperature of 200 °C.

Sample	B_1[%]	τ_1[ns]	B_2[%]	τ_2[ns]	τ_{avg}[ns]
r-CDs	91	0.84	9	2.73	1.00

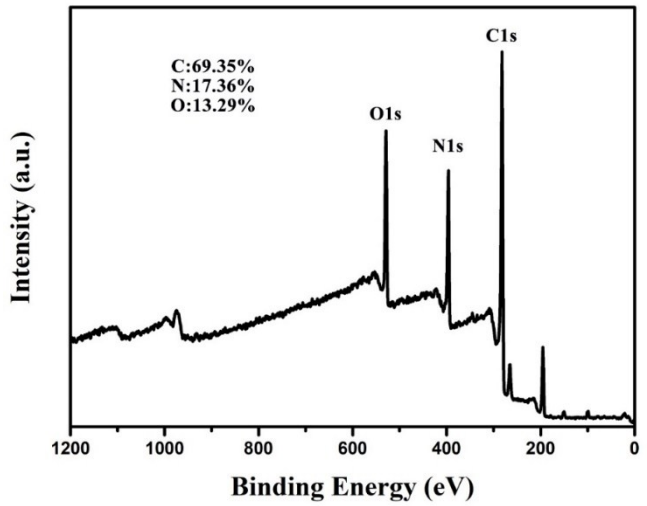

Figure S4. Survey of XPS spectra of r-CDs during the calcination treatment for 6 h at the temperature of 200 °C.

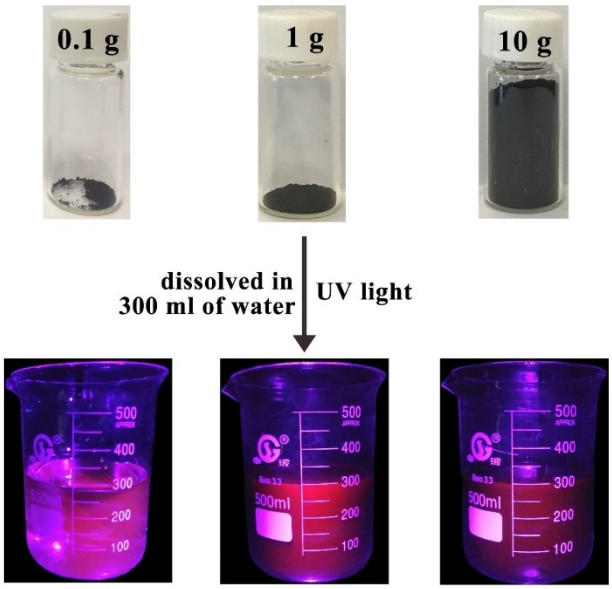

Figure S5. Schematic illustration of large-scale preparation of solid-state r-CDs.

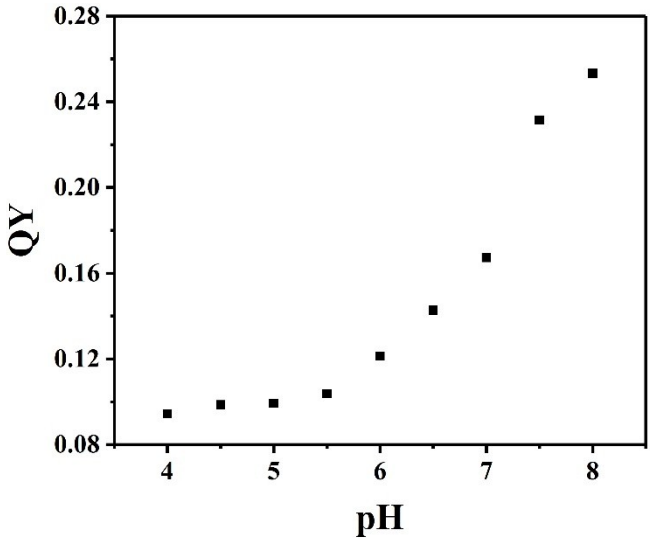

Figure S6. The QYs of CDs at different pH values.

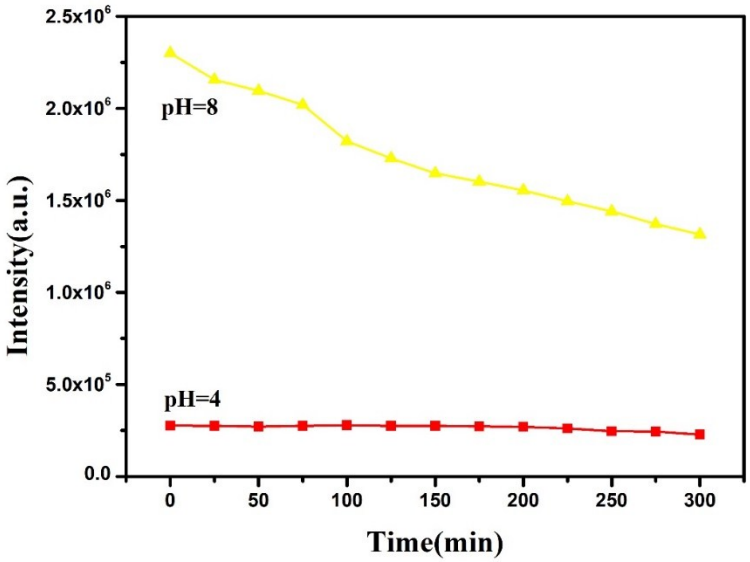

Figure S7. Photostability of r-CDs at different pH values over 5 h of UV irradiation.

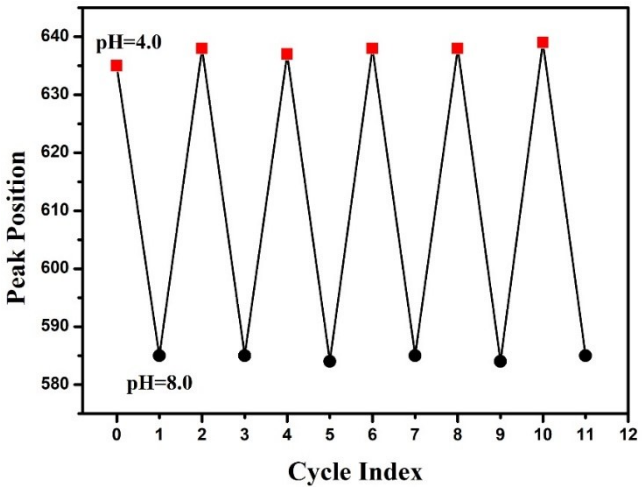

Figure S8. Fluorescence reversibility of r-CDs at different pH values.

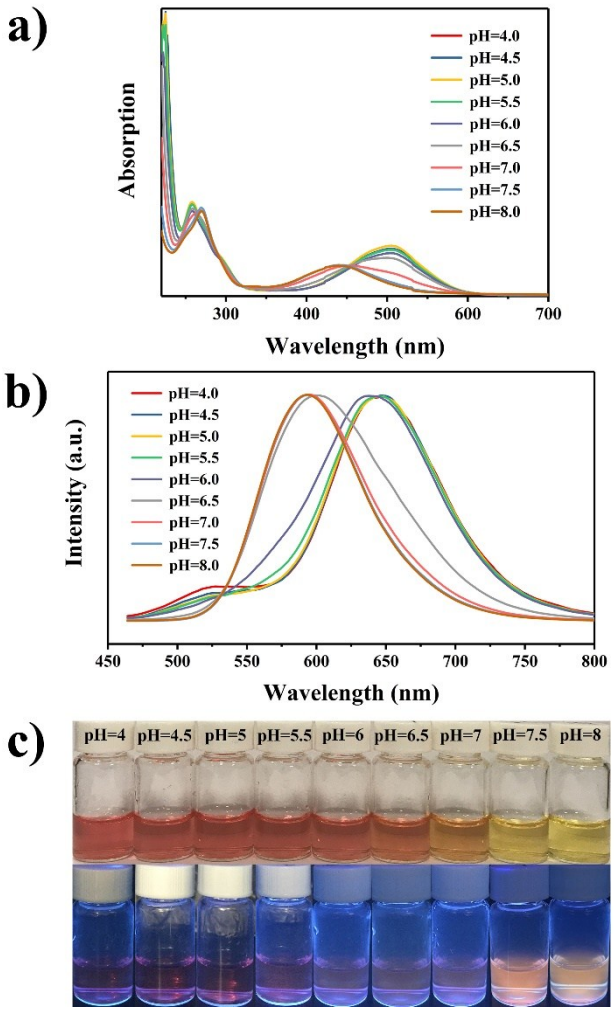

Figure S9. The colorimetric and fluorometric pH response of CDs-1 from 1,2,4-triaminobenzene by the hydrothermal method. a) UV-vis absorption spectrum and b) PL spectra of CDs-1 at different pH values under excitation of 444 nm, c) photos of CDs-1 at different pH values in daylight (upper) and UV light (bottom).

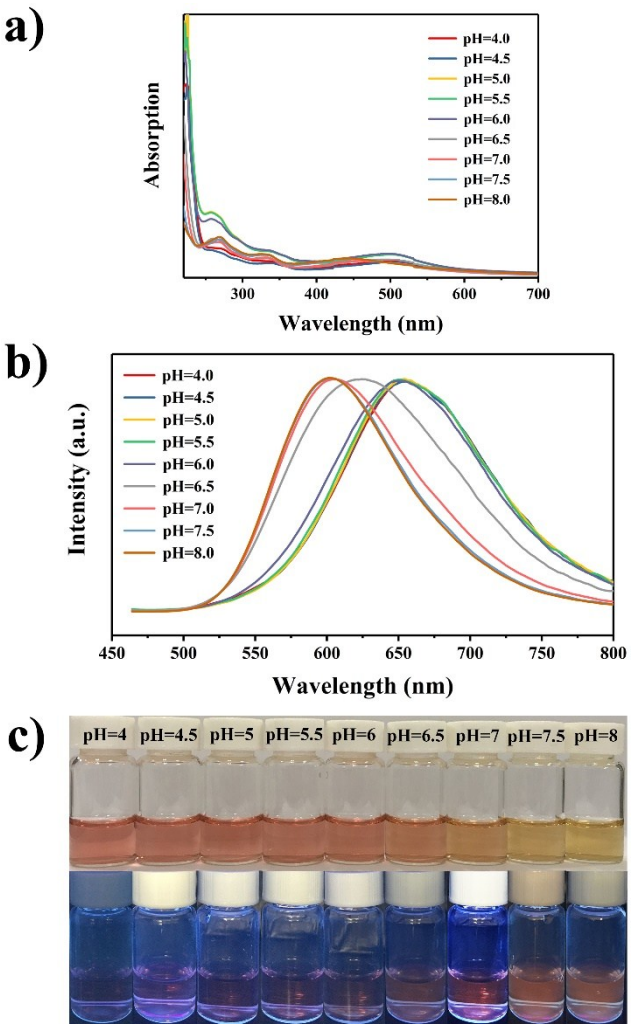

Figure S10. The colorimetric and fluorometric pH response of CDs-2 from 1,2,4-triaminobenzene by the microwave method. a) UV-vis absorption spectrum and b) PL spectra of CDs-2 at different pH values under excitation of 444 nm, c) photos of CDs-2 at different pH values in daylight (upper) and UV light (bottom).

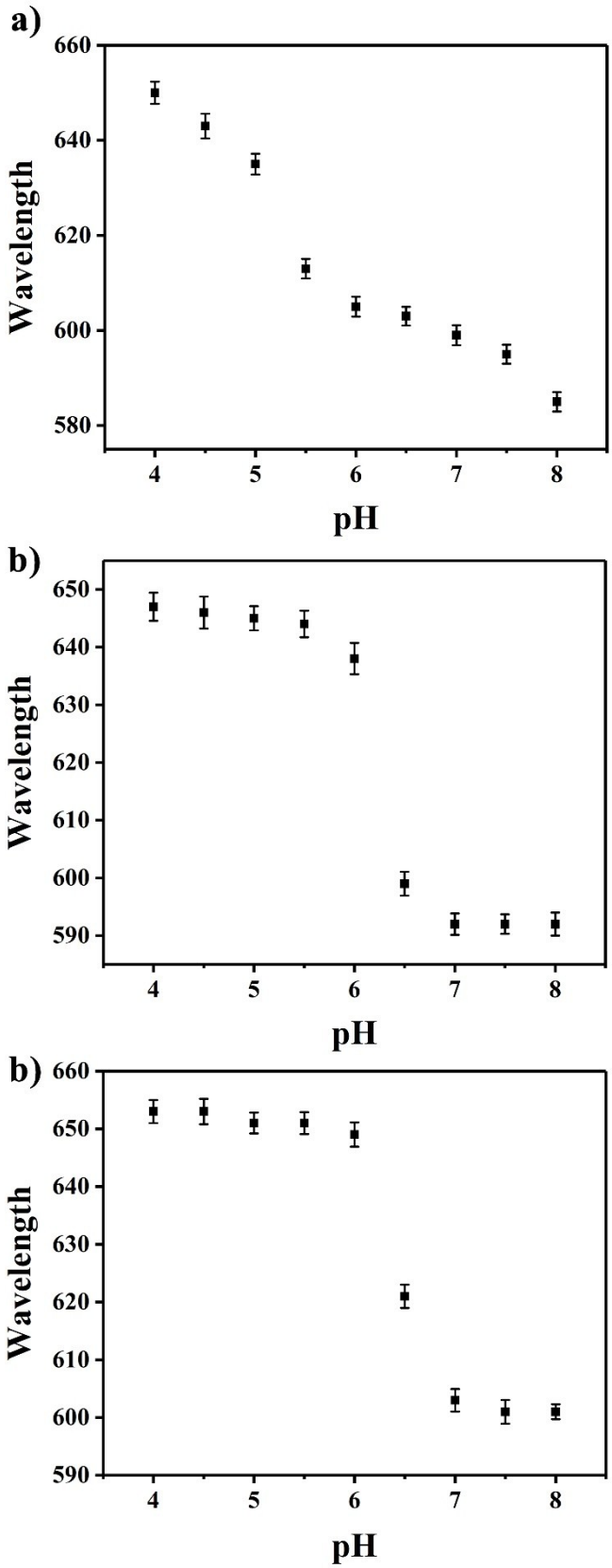

Figure S11. The emission wavelength changes of three kinds of CDs with pH respectively by a) solid-phase synthesis, b) hydrothermal method and c) microwave method.

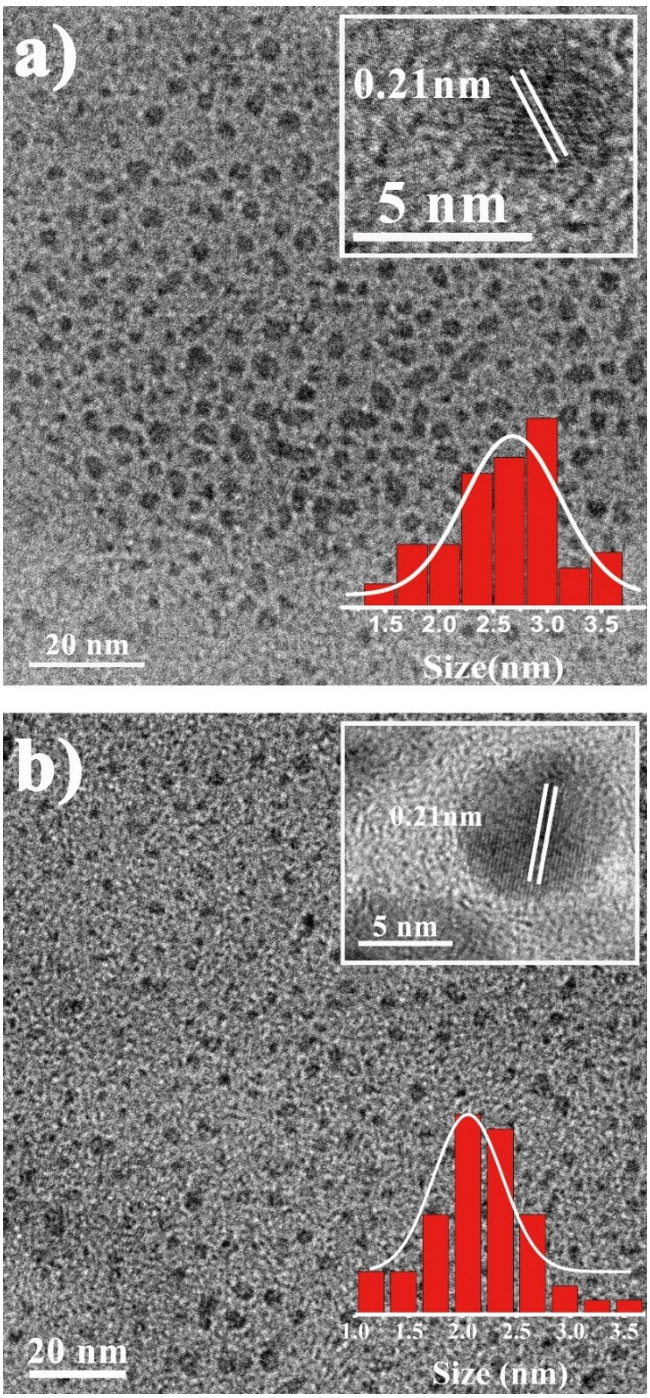

Figure S12. TEM images of r-CDs at a) pH=4.0 and b) pH=8.0. Inserts: HRTEM images (top) and size distribution histograms (bottom) of the r-CDs at pH=4.0 and pH=8.0, respectively.

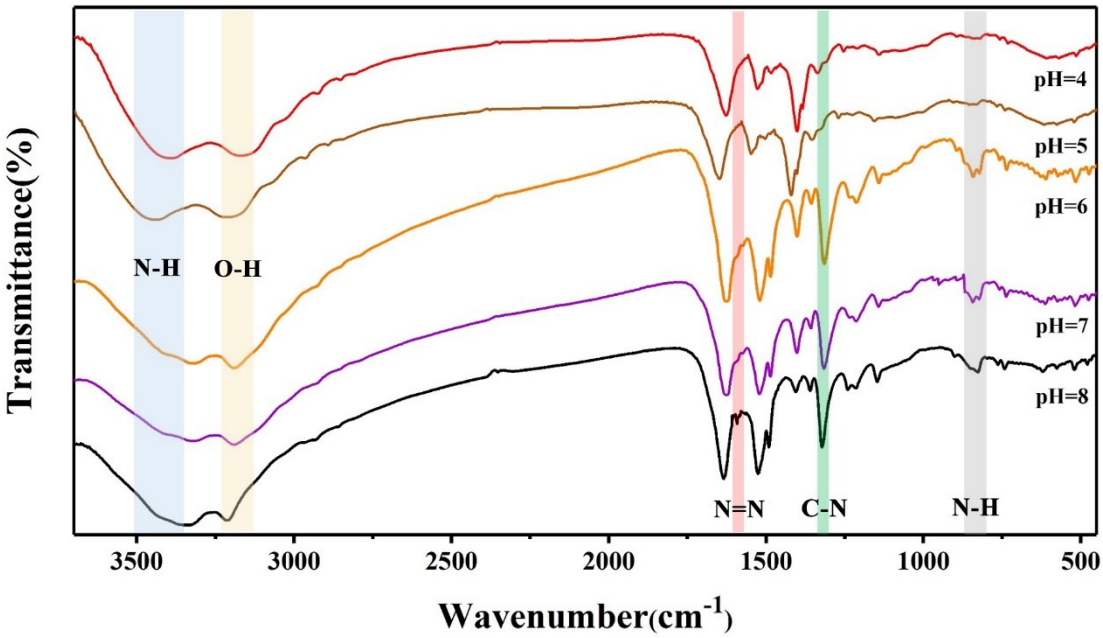

Figure S13. The FT-IR spectrum of r-CDs at different pH values.

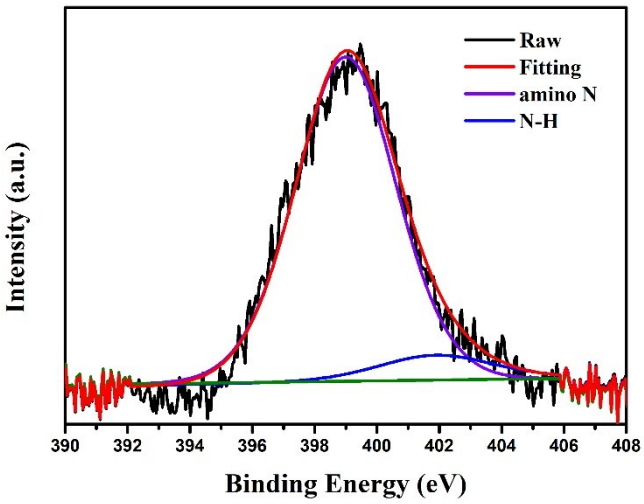

Figure S14. The high-resolution XPS spectrum of N 1s of r-CDs at pH 8.0.

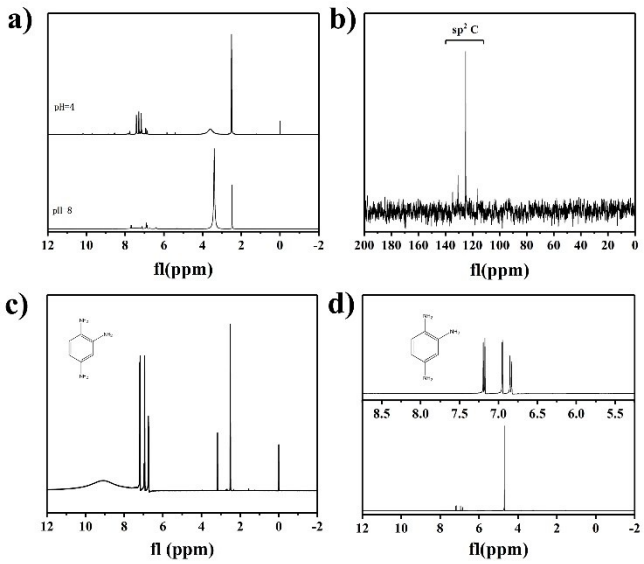

Figure S15. (a) ^{1}H NMR spectrum of r-CDs in DMSO-d_6 (10 mg/mL); (b) ^{13}C NMR spectrum of r-CDs in D_2O (40 mg/mL); (c) and (d) ^{1}H NMR spectrum of 1,2,4-triaminobenzene in DMSO-d_6 and D_2O (10 mg/mL).

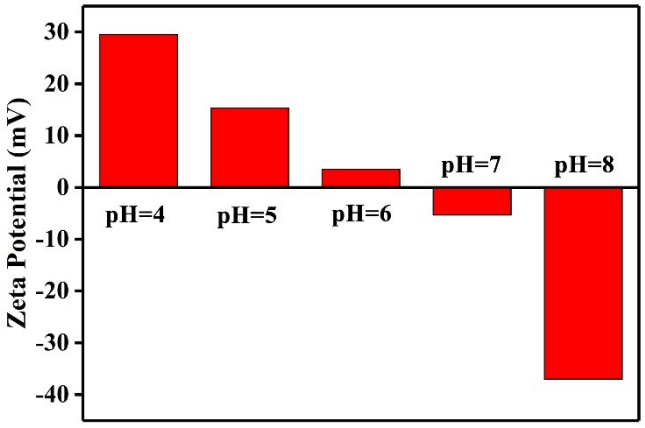

Figure S16. Zeta potentials of r-CDs at different pH values.

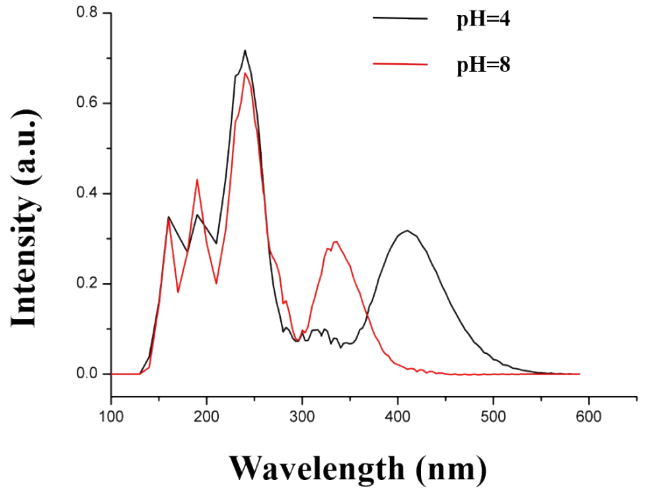

Figure S17. Simulated absorption spectra at optimized S_0 geometry of r-CDs at different pH.

Table S2. Calculated lowest-lying singlet absorption (λ, nm), oscillator strength (*f*), and transition property of r-CDs at different pH.

	λ(nm)	*f*	transition	contribution (%)
pH=4	410	0.5301	HOMO → LUMO	97
pH=8	337	0.5119	HOMO → LUMO	95

The molecular structures of ground state were optimized at the density functional theory (DFT) using the M06-2X method. [1,2] In all calculations, the triple-ζ basis sets augmented with polarization functions (def2-TZVP) was employed in Gaussian 09 program. [3,4]

[1] R.G. Parr, Density functional theory of atoms and molecules, Horizons of Quantum Chemistry, (1980) 5-15.

[2] Y. Zhao, D.G. Truhlar, The M06 suite of density functionals for main group thermochemistry, thermochemical kinetics, noncovalent interactions, excited states, and transition elements: two new functionals and systematic testing of four M06-class functionals and 12 other functionals, Theoretical Chemistry Accounts 120(1-3) (2008) 215-241.

[3] F. Weigend, R. Ahlrichs, Balanced basis sets of split valence, triple zeta valence and quadruple zeta valence quality for H to Rn: Design and assessment of accuracy, Phys. Chem. Chem. Phys. 7(18) (2005) 3297-3305.

[4] M.J. Frisch, G. Trucks, H. Schlegel, G. Scuseria, M. Robb, J. Cheeseman, G. Scalmani, V. Barone, B. Mennucci, G. Petersson, Gaussian 09, Revision D. 01, Gaussian, Inc.: Wallingford, CT (2009)

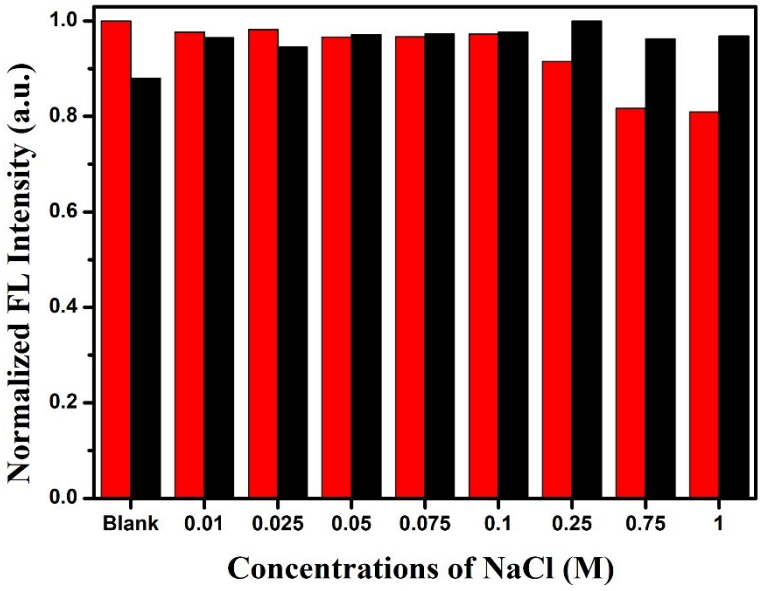

Figure S18. FL intensity variation of the r-CDs as concentrations of NaCl (red bar

represents pH=4 and black bar represents pH=8).

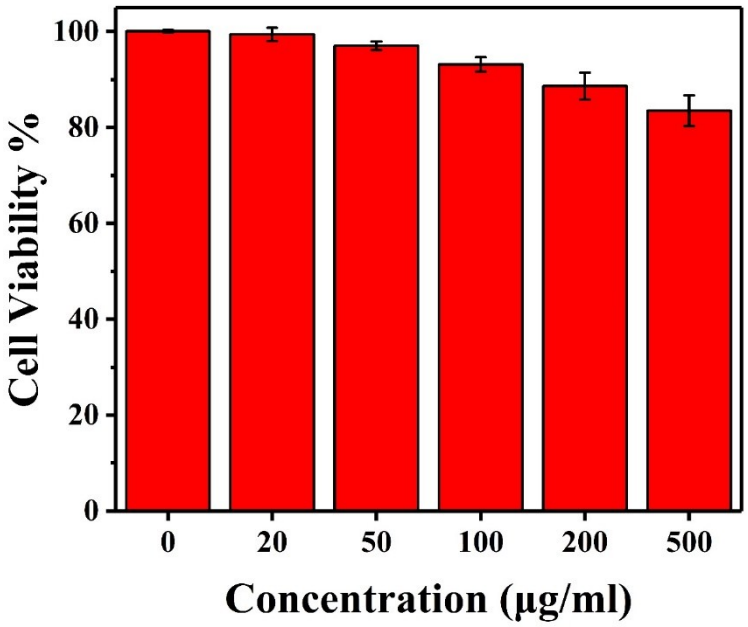

Figure S19. Cell viability of Hela cells with different concentrations of r-CDs.